Mutational Analysis of an RNA Internal Loop as a Reactivity Epitope for *Escherichia coli* Ribonuclease III Substrates†

Irina Calin-Jageman and Allen W. Nicholson*

Department of Biological Sciences, Wayne State University, Detroit, Michigan 48202

Received January 3, 2003; Revised Manuscript Received March 5, 2003

ABSTRACT: The enzymatic cleavage of double-stranded (ds) RNA is an obligatory step in the maturation and decay of many cellular and viral RNAs. The primary agents of dsRNA processing are members of the ribonuclease III (RNase III) superfamily, which are highly conserved in eukaryotic and bacterial cells. *Escherichia coli* RNase III participates in the maturation of the ribosomal RNAs and in the maturation and decay of cellular and phage mRNAs. *E. coli* RNase III-dependent cleavage events can regulate gene expression by controlling mRNA stability and translational activity. RNase III recognizes its substrates and selects the scissile phosphodiester(s) by recognizing specific RNA sequence and structural elements, termed reactivity epitopes. Some *E. coli* RNase III substrates contain an internal loop, in which is located the single scissile phosphodiester. The specific features of the internal loop that establish the pattern of single-strand cleavage are not known. A mutational analysis of the asymmetric [4 nt/5 nt] internal loop of the phage T7 R1.1 substrate reveals that cleavage reactivity is largely independent of internal loop sequence. Instead, the [4/5] asymmetry per se is the primary determinant of cleavage of a single bond within the 5 nt strand of the internal loop. The T7 R1.1 internal loop lacks elements of local tertiary structure, as revealed by sensitivity to cleavage by terbium ion and by the ability of the internal loop to destabilize a small model duplex. The internal loop functions as a discrete structural element in that the pattern of cleavage can be controlled by the specific type of asymmetry. The implications of these findings are discussed in light of RNase III substrate function as a gene regulatory element.

Ribonucleases are essential participants in the formation and decay of cellular and viral RNAs and provide the enzymatic basis of diverse posttranscriptional regulatory mechanisms. Endonucleolytic or exonucleolytic cleavage reactions can establish mRNA half-lives and translational efficiencies, as well as provide mononucleotides for new RNA synthesis (*1*−*5*). The activities of cellular ribonucleases are regulated at a variety of levels, which is in part necessitated by the need to avoid inadvertent, potentially deleterious cleavage events.

Specific RNA structural and sequence elements provide signals for substrate recognition and cleavage site selection. Double-stranded RNA (dsRNA)[1] structures are targets for cleavage by members of the ribonuclease III superfamily (*6*). Eukaryotic RNase III orthologues are involved in rRNA, snoRNA, and snRNA maturation (*6*, *7*), and the structurally and functionally distinct orthologue Dicer is an integral component of the RNA interference (RNAi) pathway. Dicer cleaves dsRNAs to create small (21−23 bp) duplexes, termed small interfering (si) RNAs, which in turn direct the enzymatic destruction of homologous RNA sequences (*8*). Dicer also cleaves precursors to microRNAs, directly providing the mature species that exert cistron-specific translational control (*9*, *10*).

RNase III is highly conserved in the bacteria, with *Escherichia coli* RNase III the most studied orthologue (*11*−*13*). *E. coli* RNase III cleaves ribosomal RNA precursors and participates in the maturation and decay of other specific cellular and phage mRNAs (*11*, *12*). *E. coli* RNase III substrates typically contain a dsRNA element of ∼20 bp, with cleavage occurring on both strands of the target site to provide products with 2 nt 3′-overhangs (*11*, *12*, *14*, *15*). RNase III primarily recognizes its substrates at two specific regions, termed the proximal box and distal box. The presence of specific Watson−Crick (W−C) bp sequences within either of the two boxes can inhibit binding of RNase III (*16*). These inhibitory W−C bp sequences are proposed to act as antideterminants, which participate in cleavage site selection and also protect other RNAs from unwanted cleavage (*12*, *16*). The sensitivity to position-specific W−C bp also is compatible with the known ability of *E. coli* RNase III to cleave dsRNAs of broad sequence complexity (*11*, *14*, *15*).

RNA internal loops provide an additional type of reactivity epitope for *E. coli* RNase III substrates and function to constrain cleavage to a single phosphodiester within the internal loop. Bacteriophage T7 expresses a number of transcripts containing RNase III substrates with internal loops. The substrates occupy intercistronic positions within the T7 early and late genetic regions (Figure 1), and site-specific single-strand cleavage directly provides the mature, fully functional

† Research supported by NIH Grant GM56772.

* To whom correspondence should be addressed at the Department of Chemistry, Temple University, 1901 N. 13th St., Philadelphia, PA 19122. Phone: 215-204-4410. Fax: 215-204-1532. E-mail: anichol@temple.edu.

[1] Abbreviations: bp, base pair; dsRNA, double-stranded RNA; IL, internal loop; nt, nucleotide; RNase III, ribonuclease III; W−C, Watson−Crick.

10.1021/bi030004r CCC: $25.00
Published on Web 04/09/2003

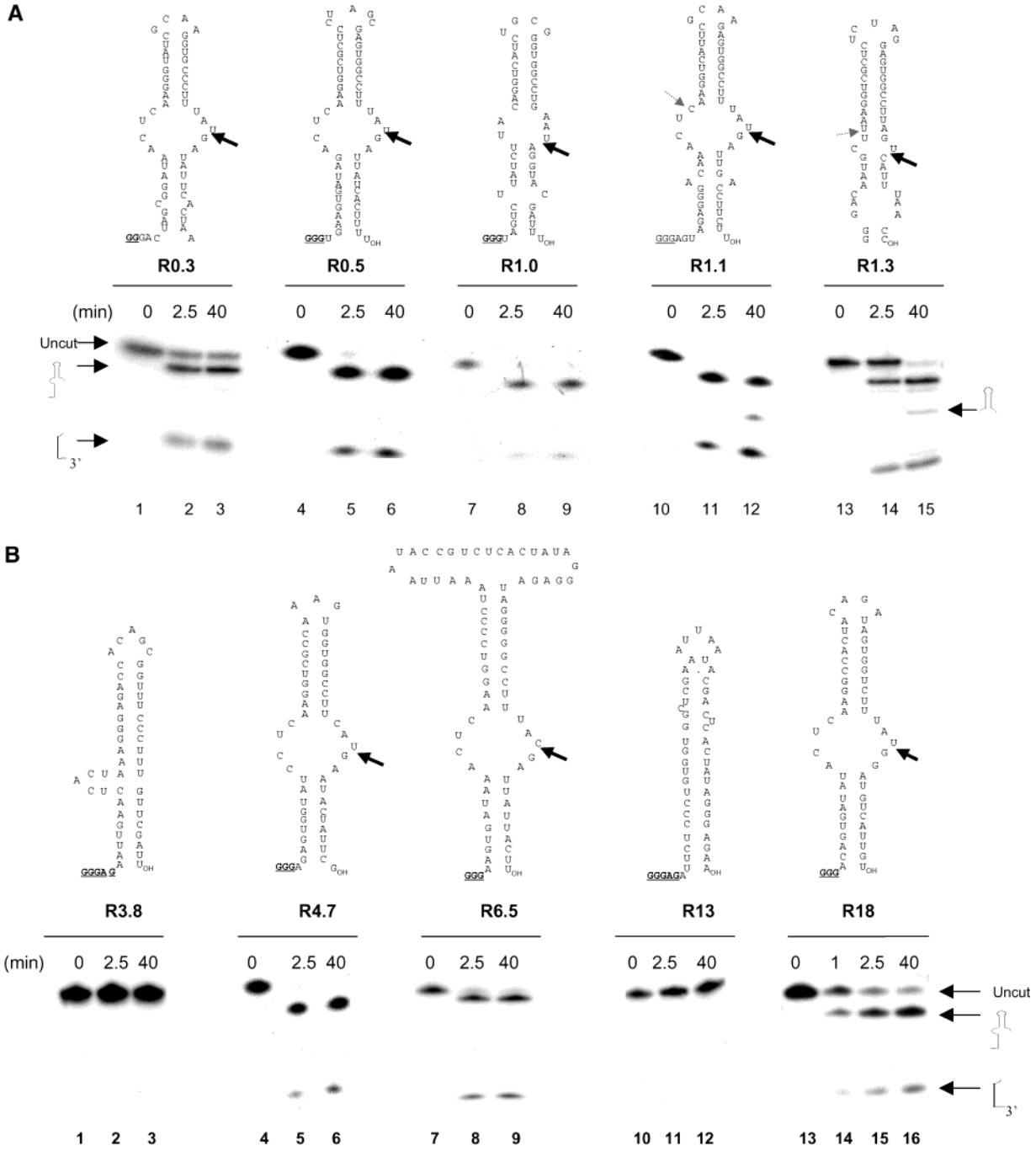

FIGURE 1: Bacteriophage T7 RNase III processing substrates. (A) Structures and cleavage reactivities of RNase III substrates in the T7 genetic early region. Shown are the sequences and secondary structures of the RNAs used in this study (see Results). The structures are essentially the same as presented previously (*18*) and are also consistent with an Mfold analysis (I. Calin-Jageman and A. W. Nicholson, unpublished). The primary RNase III cleavage sites are indicated by the arrows. The secondary cleavage sites in the R1.1 and R1.3 substrates are indicated by the small dashed arrows. The non-T7-encoded nucleotides at the 5′ end are underlined. Cleavage assays involved incubation of internally ^{32}P-labeled substrate with RNase III for the indicated times, followed by electrophoresis in a 15% polyacrylamide gel containing 7 M urea (see Experimental Procedures). The left side of the panel indicates the position of uncleaved substrate and the two products of cleavage at the primary site. Indicated on the right side of the panel is the main product of cleavage at the primary and secondary sites of R1.1 RNA and R1.3 RNA. (B) Structures and cleavage reactivities of proposed RNase III substrates in the T7 middle and late genetic regions. Cleavage assays were carried out as described above and in Experimental Procedures.

mRNAs (*17*, *18*). In particular, cleavage within the 3′ segment of the internal loops provides 3′-hairpins, which contribute to the prolonged physical half-lives of the T7 mRNAs (*18*, *19*). Other 3′-end hairpin structures are known to stabilize bacterial RNAs (*20*, *21*). While there is an established function for single-strand cleavage within an internal loop, the sequence and/or structural features of the T7 internal loops that are responsible for the particular pattern of cleavage are not known. We present here a mutational analysis of an internal loop present in T7 RNase III substrates and describe the important features that define the pattern of cleavage.

EXPERIMENTAL PROCEDURES

Materials. Water was deionized and distilled. Chemicals were of molecular biology grade and were purchased from

Fisher Scientific or Sigma. *E. coli* bulk stripped tRNA was purchased from Sigma and was further purified by repeated phenol extraction and ethanol precipitation. Radiolabeled nucleotides [γ-^{32}P]ATP (3000 Ci/mmol), [α-^{32}P]CTP (3000 Ci/mmol), and [α-^{32}P]UTP (3000 Ci/mmol) were obtained from Perkin-Elmer. Standardized 1 M $MgCl_2$ and $TbCl_3$ were obtained from Sigma. Oligodeoxynucleotide transcription templates were synthesized by the Wayne State Macromolecular Core Facility or by Invitrogen and were purified by denaturing gel electrophoresis as described (*22*). Chemically synthesized RNA oligonucleotides were provided by Dharmacon and were further purified by gel electrophoresis. Calf intestinal alkaline phosphatase was purchased from Roche Molecular Biochemicals, and T4 polynucleotide kinase was obtained from New England Biolabs. T7 RNA polymerase was purified from an overexpressing bacterial strain as described (*23*, *24*). RNase III was purified as an N-terminal $(His)_6$-tagged protein from an overproducing bacterial strain (*22*).

Substrate Synthesis. RNase III substrates were prepared by transcription of oligodeoxynucleotide templates as described (*22*). RNA was internally ^{32}P-labeled by including [α-^{32}P]CTP or [α-^{32}P]UTP (3−15 μCi) along with the four unlabeled nucleotides in the transcription reactions. RNA was 5′-^{32}P-labeled by incubating calf alkaline phosphatase-treated, unlabeled transcript with T4 polynucleotide kinase and 3−10 μCi of [γ-^{32}P]ATP (3000 Ci/mmol) (*22*). Radiolabeled RNAs were purified by denaturing gel electrophoresis as described (*22*) and stored at −20 °C in Tris−EDTA buffer (pH 7).

Substrate Cleavage Assay. Cleavage assays were carried out as described (*22*) using internally or 5′-^{32}P-labeled RNA. To remove intermolecular aggregates formed during storage at −20 °C, substrate was heated at 100 °C for 30 s in TE buffer and then snap-cooled on ice. The reaction buffer contained 250 mM potassium glutamate (or 160 mM NaCl), 10 mM $MgCl_2$, 30 mM Tris-HCl (pH 8), 0.1 mM EDTA, 0.1 mM DTT, 0.01 mg/mL tRNA, and 5% (v/v) glycerol. Reactions were initiated by addition of $MgCl_2$ and quenched by the addition of a stop mix containing 20 mM EDTA (*22*). Samples were electrophoresed in a denaturing 15% polyacrylamide gel containing 7 M urea and TBE buffer (*22*). Visualization of the reactions was carried out by phosphorimaging (Molecular Dynamics Storm 860 system), and reactions were quantitated using ImageQuant software.

RESULTS

Comparison of in Vitro Cleavage Reactivities of T7 Early and Late RNase III Substrates. The T7 chromosome encodes a set of RNase III substrates that occupy intercistronic positions within the early and late genetic regions (Figure 1) (*18*). The T7 RNase III substrate structures are hairpin stem−loops, most of which contain an asymmetric internal loop in which is located the single site of cleavage (Figure 1). The primary transcription products undergo cleavage at these sites to provide the mature, fully functional mRNAs. The five T7 early processing signals (R0.3, R0.5, R1.0, R1.1, and R1.3) (Figure 1A) are present within the ∼7000 nt polycistronic early mRNA precursor which is synthesized by the host RNA polymerase and is cleaved during transcription (*18*). The T7 R1.1 genetic element has provided a relevant model with which to determine structure−reactivity correlates of *E. coli* RNase III substrates (*16*, *25*−*28*, *29*).

The T7 late RNase III substrates (Figure 1B) have not been biochemically characterized, and the reactivities of two of them (R3.8 and R13) are in question (*18*). To gain more information on internal loop function as a reactivity epitope, small RNAs were enzymatically synthesized to contain the sequences of the five T7 early RNase III substrates and the five proposed T7 late substrates. Internally ^{32}P-labeled transcripts were assessed for their cleavage reactivities in vitro using purified RNase III and physiologically relevant salt and Mg^{2+} concentrations. Consistent with previous studies, all five early substrates undergo cleavage at a single site (Figure 1A). Additional assays (data not shown) indicate that the eight substrates are cleaved at comparable rates. A small amount of cleavage was observed at the secondary cleavage sites in R1.1 RNA and R1.3 RNA (Figure 1A, lanes 12 and 15; indicated by the small dashed arrows in the diagrams).

Three of the late substrates (R4.7, R6.5, and R18 RNA) also undergo cleavage. However, the proposed substrates R3.8 RNA and R13 RNA are not detectably cleaved, even at extended reaction times (Figure 1B, lanes 1−3 and 10−12) or at high enzyme concentrations (data not shown). The cleavage resistance is consistent with the negligible in vivo reactivities of plasmid-encoded transcripts containing these sequences (*18*). We conclude that R3.8 RNA and R13 RNA are not RNase III substrates. The cleavage sites in R4.7, R6.5, and R18 RNA were mapped by sequencing gel analysis of RNase III-treated 5′-^{32}P-labeled RNA, using a base-specific P1 nuclease digestion ladder as reference (data not shown but see legend to Figure 2). For each substrate the cleavage site is 5′ to the G residue in the 3′-end proximal segment of the internal loop (indicated by the solid arrows in Figure 1B). The cleavage sites of the T7 late substrates agree with the predictions based on secondary structure comparison (*18*). The R4.7, R6.5, and R18 RNase III substrates formally possess a [4/5] internal loop which is structurally identical to the R0.3, R0.5, and R1.1 internal loops. We conclude that T7 RNase III substrates with a [4/5] internal loop exhibit a conserved pattern of single-strand cleavage.

The T7 R1.1 Internal Loop Lacks Elements of Local Tertiary Structure. An imino proton NMR analysis of R1.1 RNA did not reveal stable hydrogen bonds localized to the internal loop (*28*), indicating the lack of stable local folding. However, the R1.1 internal loop may possess a defined structure stabilized by interactions not involving hydrogen bonds. To examine this possibility, we used terbium ion (Tb^{3+}) as a structural probe. It has been shown that RNA phosphodiesters in unstructured regions are cleaved by Tb^{3+} in a sequence-independent manner (*30*, *31*). 5′-^{32}P-labeled R1.1 RNA was incubated with Tb^{3+}, and the products were analyzed by sequencing gel electrophoresis. A representative assay is shown in Figure 2A. Tb^{3+}-sensitive sites are observed in the internal loop 3′ segment (IL-3′) and 5′ segment (IL-5′), as well as in the hairpin tetraloop (Figure 2A, lanes 3 and 4; summarized in Figure 2B). For comparison we also examined the Tb^{3+} reactivity of R1.1[WC-R] RNA (Figure 2B), which is a fully W−C base-paired variant of R1.1 RNA (*27*). For this RNA, the phosphodiesters corresponding to the internal loop region are uniformly unreactive (Figure 2A, compare lanes 6 and 7 with lanes 3 and 4; summarized in Figure 2B). In summary, the Tb^{3+} reactivity pattern of R1.1 RNA is consistent with the occurrence of an unstructured internal loop.

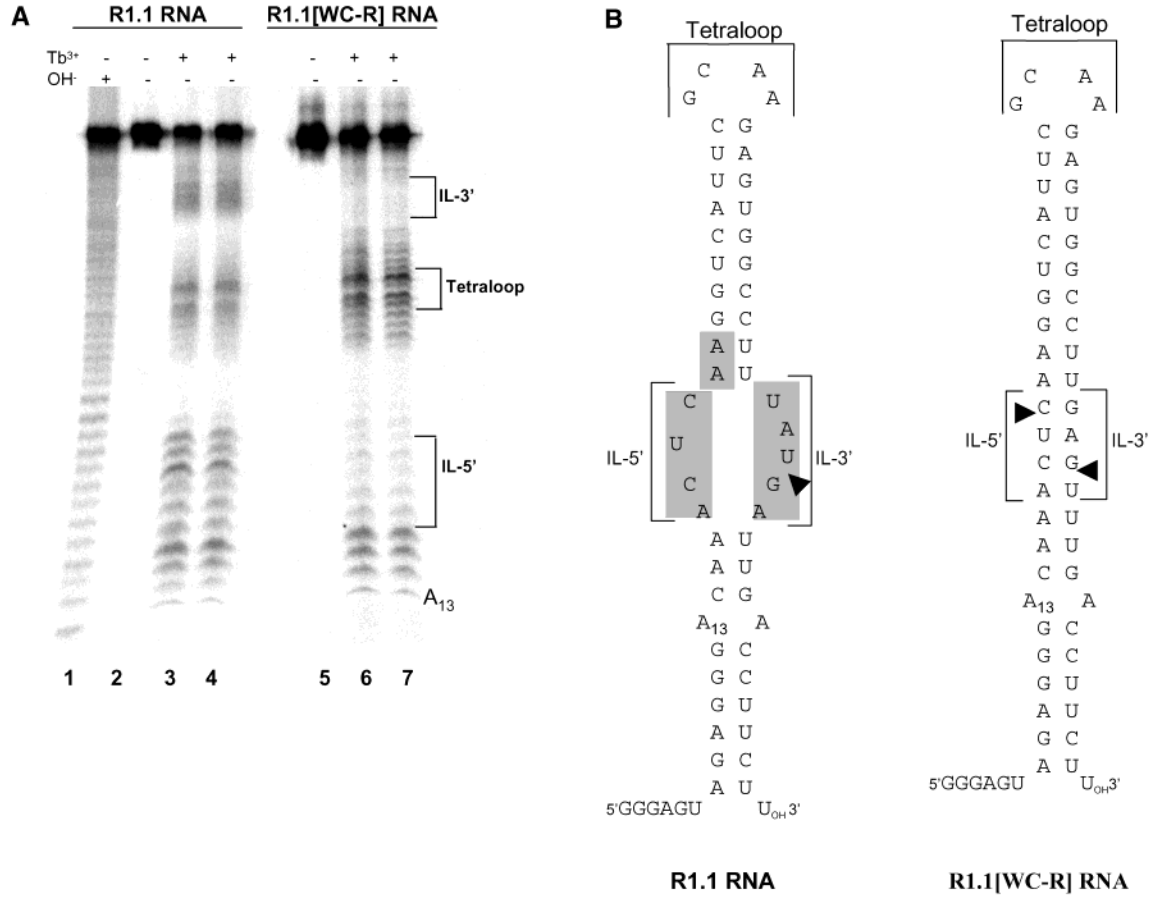

FIGURE 2: The R1.1 internal loop lacks stable tertiary structure as revealed by terbium ion reactivity. (A) Tb^{3+} ion cleavage patterns. R1.1 RNA and R1.1[WC-R] RNA were 5′-^{32}P-labeled as described in Experimental Procedures and were incubated at 37 °C in the presence of 5 mM Tb^{3+} (lanes 3, 4, 6, and 7) or in the absence of Tb^{3+} (lanes 2 and 5). Aliquots were electrophoresed (1400 V) in a 2 mm thick 10% polyacrylamide gel containing 7 M urea and the reactions visualized by phosphorimaging. Cleavage sites were assigned by a separate gel electrophoretic analysis (data not shown), involving comparison of cleavage products with those from a nuclease P1 digestion (G-specific) (*54*). An alkaline ladder (lane 1) was generated by heating 5′-^{32}P-labeled R1.1 RNA in 0.5 mM sodium carbonate (pH 9.2) at 90 °C for 10 min. The regions of the cleavage pattern corresponding to the tetraloop and the internal loop 3′ segment and 5′ segment are indicated. (B) Mfold-based structures of R1.1 RNA and R1.1[WC-R] RNA. The shaded regions in R1.1 RNA indicate the Tb^{3+}-sensitive nucleotides specific to that substrate. Nucleotide A13 is specifically identified to allow correlation with the data in panel A.

It is expected that an unstructured internal loop would destabilize a double helix. To test this, we analyzed the formation and stability of a small duplex containing the R1.1 internal loop sequence. A 16 nt RNA containing the sequence of the internal loop 5′ segment and flanking nucleotides (R1.1[IL5′] RNA) was combined with a 17 nt RNA containing the sequence of the internal loop 3′-segment and flanking nucleotides (R1.1[IL3′] RNA) (Figure 3A). A second duplex was prepared that instead exhibited full W−C base pairing, which was obtained by combining R1.1[IL5′] RNA with the fully complementary sequence, R1.1[WC3′] RNA (Figure 3B). In each experiment, 5′-^{32}P-labeled R1.1[IL5′] RNA was incubated with the specified amounts of unlabeled R1.1[IL3′] RNA or R1.1[WC3′] RNA, and complex formation was monitored by electrophoresis in a nondenaturing polyacrylamide gel. In each experiment a species of reduced electrophoretic mobility was observed (panels A and B of Figure 3, lanes 2−6), indicative of complex formation. The amount of complex formed was a function of the amount of added complementary RNA.

To assess the general structural features of the two complexes, aliquots of the annealing reactions were treated with pancreatic ribonuclease prior to electrophoresis. The complex designed to contain full W−C base pairing was insensitive to RNase, whereas the complex containing the R1.1 internal loop sequence was cleaved (data not shown). The ribonuclease sensitivity of the latter complex is consistent with the presence of an unstructured internal loop containing several pancreatic ribonuclease-sensitive pyrimidines.[2]

RNA titration experiments were performed to obtain the apparent dissociation constant (K'_D) for each complex (Figure 3). The K'_D of the R1.1 internal loop-containing complex is 76 nM, while the K'_D of the fully W−C base-paired complex is 0.9 nM. The K'_D values show that the complex with the R1.1 internal loop sequence is significantly less stable than the fully base-paired complex, with the 84-fold difference corresponding to a free energy difference ($\Delta\Delta G$) of ~2.6 kcal/mol (see Discussion).

R1.1 RNA Cleavage Reactivity Does Not Strictly Depend on the Consensus Internal Loop Sequence. The [4/5] internal loops of six of the eight T7 RNase III substrates (R0.3, R0.5,

[2] The RNase III cleavage reactivities of the two complexes were not examined since they were of insufficient size for enzyme recognition.

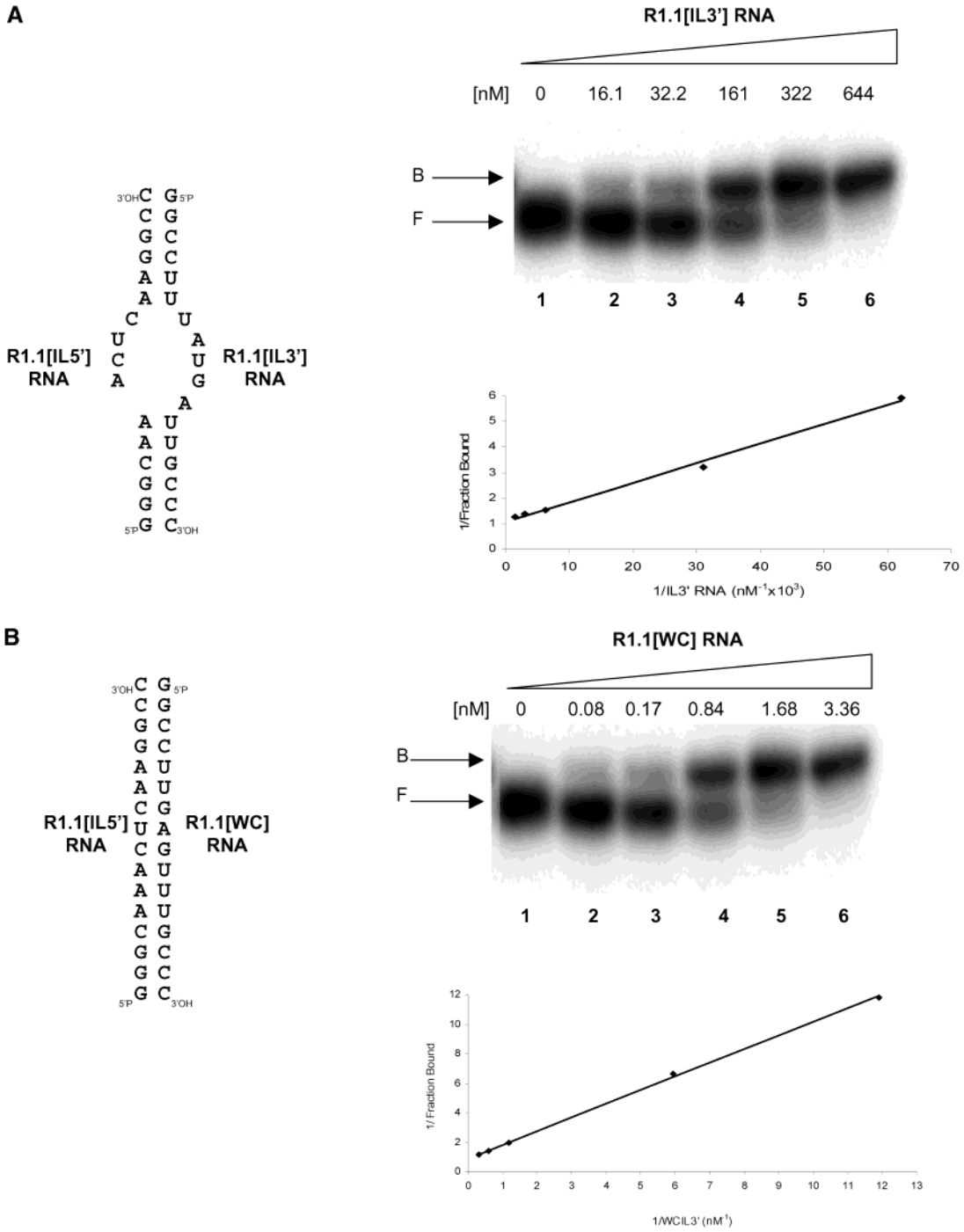

FIGURE 3: The R1.1 internal loop destabilizes a small model duplex. (A) Analysis of the R1.1 internal loop-containing complex. The left-hand side of the panel shows the proposed structure of the intermolecular complex of R1.1[IL5′] RNA and R1.1[IL3′] RNA. The two RNAs were chemically synthesized, then deprotected, and gel purified. R1.1[IL-5′] RNA was 5′-^{32}P-labeled as described in Experimental Procedures. RNAs were incubated at 65 °C for 5 min in buffer consisting of 160 mM NaCl and 10 mM Tris-HCl (pH 8), then incubated at room temperature for 10 min, and placed on ice. Prior to electrophoresis, glycerol was added (final concentration 1%), and the samples were electrophoresed (120 V for 3 h at 4−5 °C) in a 6% polyacrylamide gel [80:1 acrylamide:bis(acrylamide)] containing TBE buffer. Reactions were visualized by phosphorimaging. The top right-hand panel shows a representative analysis. F and B indicate the positions of free and bound R1.1[IL5′] RNA, respectively. The graph in the lower right-hand side is a double-reciprocal analysis (*22*) of the binding isotherm, providing the K'_D of the complex. (B) Analysis of the fully W−C base-paired complex. The proposed structure of the intermolecular complex of R1.1[IL5′] RNA and R1.1[WC3′] RNA is shown on the left-hand side. The gel shift analysis and K'_D determination were carried out using 5′-^{32}P-labeled R1.1[IL5′] RNA and unlabeled R1.1[WC3′] RNA as described above.

R1.1, R4.7, R6.5, and R18) contain similar sequences. Five of the nine positions are identical, while two positions contain a pyrimidine and one position a purine (Figure 4A). The conservation suggests a functional importance, perhaps in conferring cleavage reactivity. To assess this, we examined the reactivity of an R1.1 RNA variant containing a sequence-randomized internal loop. R1.1[Rd4/5] RNA (Rd, randomized) represents a pool of 262144 (4^9) different sequences. An in vitro cleavage assay reveals that internally ^{32}P-labeled R1.1[Rd4/5] RNA is reactive and is cleaved in a site-specific manner (Figure 4B, lanes 5−8). On the basis of the similar denaturing gel electrophoretic mobilities of the

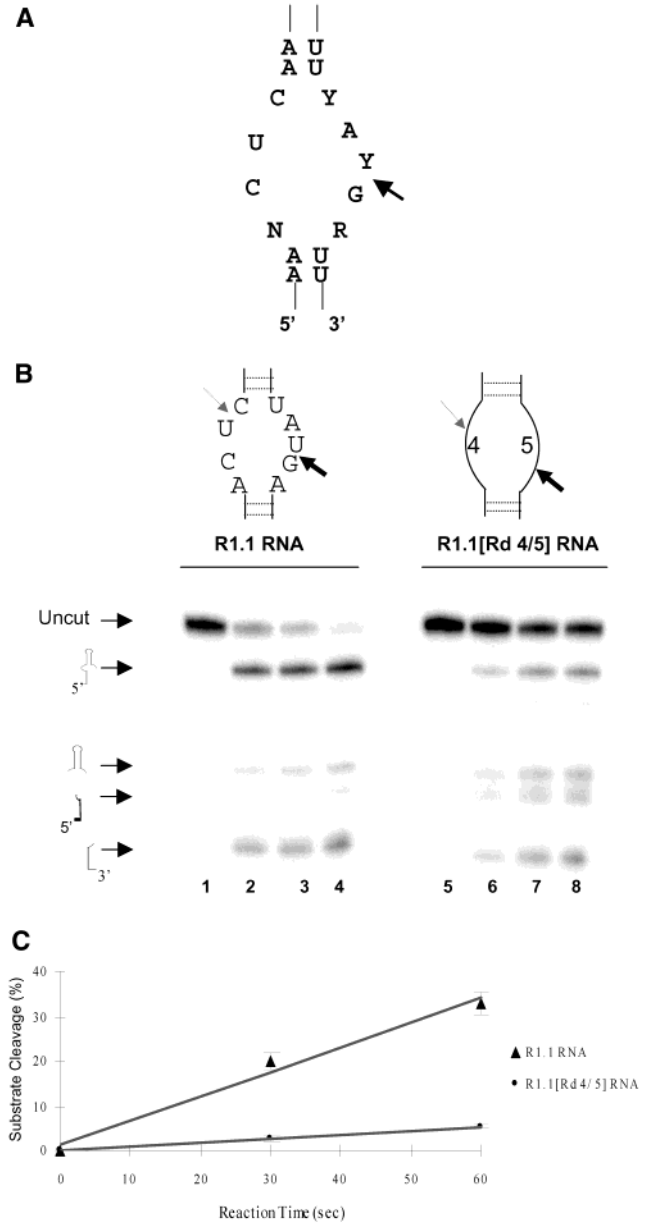

FIGURE 4: Lack of internal loop sequence requirement for substrate reactivity. (A) Consensus sequence of the [4/5] internal loop in T7 RNase III substrates. The arrow indicates the canonical RNase III cleavage site. Abbreviations: Y, pyrimidine; R, purine; N, any nucleotide. (B) Time course for RNase III cleavage of R1.1 RNA and R1.1[Rd4/5] RNA. Internally ^{32}P-labeled RNA was incubated with RNase III (9 nM) for the times given below. Samples were analyzed by polyacrylamide gel electrophoresis and phosphorimaging (see Experimental Procedures). Incubation times: lanes 2 and 6, 5 min; lanes 3 and 7, 40 min; lanes 4 and 8, 60 min. Lanes 1 and 5 display RNAs incubated for 40 min with RNase III but in the absence of Mg^{2+}. The positions of the uncut substrate and the products of cleavage at the primary site or cleavage at the primary and secondary sites are indicated on the left. The primary and secondary cleavage sites are indicated in the two diagrams by the solid and dashed arrows, respectively. (C) Relative initial rate of cleavage of internally ^{32}P-labeled R1.1 RNA and R1.1[Rd4/5] RNA. Substrate and RNase III (10 nM) were incubated for 0, 30, or 60 s and then stopped with excess EDTA. Aliquots were subjected to denaturing gel electrophoresis, and percent cleavage was determined by phosphorimaging (see Experimental Procedures). The points represent the average of three experiments.

small products, the cleavage of R1.1[Rd4/5] RNA occurs primarily at a site corresponding to the canonical scissile bond (Figure 4B, compare lanes 2−4 with lanes 6−8).[3] There also is a minor amount of cleavage at the internal loop secondary site, similar to that seen with R1.1 RNA (Figure 4B, lanes 7 and 8).

The initial rates of cleavage of R1.1 RNA and R1.1-[Rd4/5] RNA were compared (Figure 4C). R1.1[Rd4/5] RNA is cleaved 6-fold more slowly than R1.1 RNA. The 6-fold rate difference indicates that a significant fraction of the substrate pool retains a comparable level of reactivity. If all of the conserved nucleotides were required for reactivity, then only a minor fraction (~0.01%) of the substrate pool would be reactive. Additional assays measured the amount of substrate cleaved at elevated RNase III concentrations. The results (data not shown) revealed that at high (200 nM) RNase III concentrations, ~90% of R1.1[Rd4/5] RNA is cleaved. On the basis of these experiments we conclude that the consensus internal loop sequence is not absolutely required for processing reactivity or cleavage site selectivity.[4]

The [4/5] Asymmetry of the Internal Loop Is Primarily Responsible for the Specific Pattern of Single-Site Cleavage. To determine whether the specific type of asymmetry can influence the pattern of cleavage, an R1.1 RNA variant was prepared in which the internal loop was formally "rotated" by 180° about an axis normal to the helical stems. The internal loop of R1.1[IL-180] RNA exhibits [5/4] asymmetry, while retaining the parental internal loop sequence (Figure 5). A cleavage assay of internally ^{32}P-labeled R1.1[IL-180] RNA reveals that the variant is reactive, but with the single site of cleavage shifted to a new position (Figure 5, lane 2). Sequencing gel analysis of the product of RNase III cleavage of 5′-^{32}P-labeled R1.1[IL-180] RNA (data not shown) reveals that the cleavage site is located between nucleotides G20 and A21 in the 5 nt, 5′-proximal segment of the internal loop (indicated by the arrow in Figure 5). We also examined the reactivity of R1.1[Rd5/4] RNA, a sequence-randomized variant of R1.1[IL-180] RNA. The cleavage pattern of R1.1-[Rd5/4] RNA is similar to that of R1.1[IL-180] RNA, with the predominant site of cleavage occurring within the 5 nt 5′-proximal segment (Figure 5). Some cleavage also occurs at the secondary site in the 4 nt segment (indicated by the dashed arrow in Figure 5). These experiments show that the [4/5] internal loop asymmetry is the primary factor in directing cleavage of a specific phosphodiester within the 5 nt segment of the internal loop.

To assess whether asymmetric internal loop size influences the cleavage pattern, R1.1 RNA variants were prepared to contain a sequence-randomized [3/4] or [5/6] internal loop. The products of RNase III treatment of internally ^{32}P-labeled R1.1[Rd3/4] RNA and R1.1[Rd5/6] RNA were compared with those of R1.1[Rd4/5] RNA and R1.1 RNA. The results (Figure 6) show that R1.1[Rd3/4] RNA and R1.1[Rd5/6]

[3] Due to the heterogeneous nature of the sequence-randomized substrates, the precise site of cleavage could not be determined by sequencing gel analysis. However, cleavage sites could be localized to the internal loop 5′-proximal segment or the 3′-proximal segment.

[4] The complexity of the R1.1[Rd4/5] substrate did not allow a determination of whether a small number (~1−2) of the conserved residues control cleavage reactivity. It is likely that the substrate pool exhibits a broad range of reactivities. It is shown elsewhere (I. Calin-Jageman and A. W. Nicholson, submitted for publication) that the residual fraction, which is cleavage-resistant, lacks detectable affinity for RNase III. However, one variant retains an affinity comparable to that of R1.1 RNA.

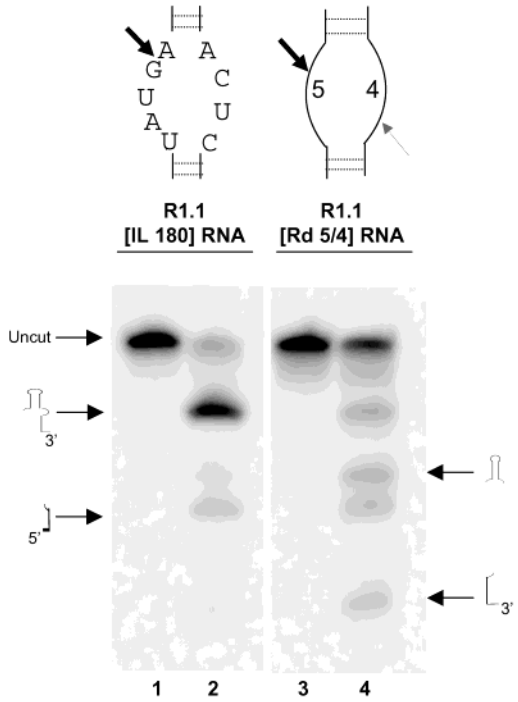

FIGURE 5: Reactivity of R1.1 RNA variants with a [5/4] internal loop. Shown at the top are the internal loop sequences of R1.1-[IL-180] RNA and R1.1[Rd5/4] RNA. Internally ^{32}P-labeled RNA was incubated with RNase III (10 nM) for 5 min at 37 °C. Samples were electrophoresed in a 15% polyacrylamide gel and visualized by phosphorimaging. Lanes 1 and 2: R1.1[IL-180] RNA. Lanes 3 and 4: R1.1[Rd5/4] RNA. Indicated on the left are the positions of the uncut substrate and the products of cleavage at the primary site (indicated by the solid arrow). On the right are indicated the products of cleavage of R1.1[IL 180] RNA at the secondary site (indicated by the dashed arrow) as well as the primary site (see text).

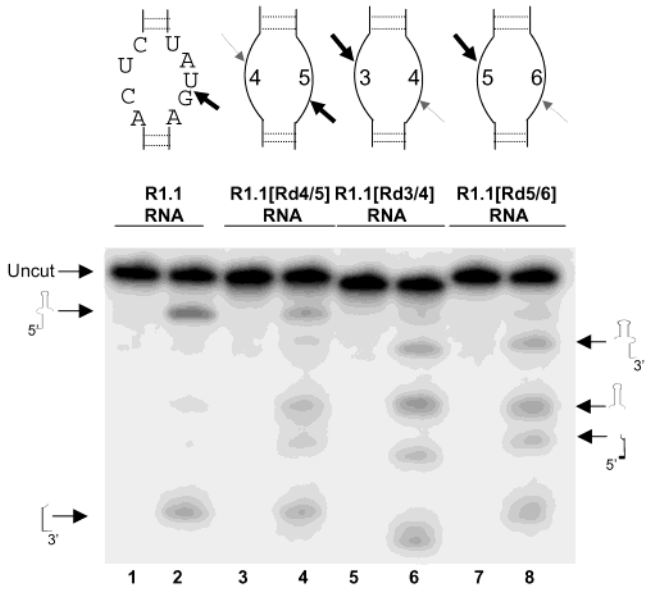

FIGURE 6: RNase III cleavage patterns of R1.1 RNA variants containing sequence-randomized asymmetric internal loops. Shown at the top are the general structures of the internal loops of R1.1 RNA, R1.1[Rd4/5] RNA, R1.1[Rd3/4] RNA, and R1.1[Rd5/6] RNA. RNAs were synthesized in internally ^{32}P-labeled form as described in Experimental Procedures. The RNAs were incubated with RNase III (10 nM) for 2.5 min at 37 °C and aliquots electrophoresed in a 15% polyacrylamide gel. On the left side of the phosphorimage are indicated the positions of the substrate and the products of cleavage at the primary site of R1.1 RNA and R1.1-[Rd4/5] RNA (see also Figure 4). On the right side are indicated the positions of the products of cleavage at the primary and secondary sites of R1.1[Rd4/5] RNA, R1.1[Rd3/4] RNA, and R1.1-[Rd5/6] RNA.

RNA are reactive. Thus, reactivity per se is not necessarily constrained to the [4/5] or [5/4] internal loop motif. However, there are qualitative differences in the cleavage pattern. On the basis of gel electrophoretic mobilities and using the known cleavage sites of R1.1 RNA and R1.1[5/4] RNA as references (see above), the gel patterns indicate that the primary site of RNase III cleavage of R1.1[Rd3/4] RNA and R1.1[Rd5/6] RNA is shifted to the 5′-proximal segment (indicated by the solid arrows in Figure 6). Thus, for both substrates there is an absence of the large product of single cleavage within the 3′-proximal segment of the internal loop (indicated on the left side of Figure 6).

The presence of the product of double cleavage (i.e., the upper stem−loop structure, indicated on the right side of Figure 6) indicates that a portion of the primary cleavage product undergoes a second cleavage event at the indicated secondary site. We conclude that, in contrast to the [3/4] and [5/6] internal loop motifs, the [4/5] internal loop directs a single cleavage event within the 3′-proximal segment.

Effect of Symmetric Internal Loops on R1.1 RNA Reactivity. Fully W−C base-paired RNase III substrates undergo cleavage on both strands, providing product ends with 2 nt 3′-overhangs (*14*, *15*, *27*). A question is whether substrates with symmetric internal loops are cleaved in a similar manner. R1.1 RNA variants containing sequence-randomized [3/3], [4/4], and [5/5] internal loops were tested for their cleavage reactivities. R1.1[Rd4/4] RNA, R1.1[Rd3/3] RNA, and R1.1[Rd5/5] RNA are all reactive (Figure 7, lanes 4, 6, and 8) and yield products resulting from cleavage of both strands of the internal loop. The product sizes are also consistent with the formation of 2 nt 3′-overhangs (see also below). The approximately equal amounts of the products of single cleavage for the three symmetric internal loop substrates indicate that neither strand is preferentially recognized.

We also examined the effect of converting the R1.1 [4/5] internal loop to a [4/4] symmetric internal loop, through deletion of a single nucleotide from the 5 nt strand. R1.1-[ΔU47] RNA and R1.1[ΔG48] RNA (Figure 8) carry a deletion of either of the two nucleotides that flank the canonical site. A cleavage assay reveals that deletion of either nucleotide promotes cleavage, similar to that seen with R1.1-[Rd4/4] RNA (Figure 8, compare lanes 4 and 6 with lanes 2 and 8). Thus, double-strand cleavage can occur even though a fully W−C base-paired structure is not possible for either variant (see top of Figure 8). Cleavage sites were mapped by sequencing gel analysis (data not shown), which reveal that when U47 is deleted, cleavage of the 3′ segment occurs between G48 and A49 (R1.1 RNA numbering), and that when G48 is deleted, cleavage occurs between U47 and A49 (R1.1 RNA numbering). The cleavage site on the opposite strand is the same for both variants, which corresponds to the R1.1 RNA secondary site (see top of Figure 8). Finally, for both R1.1 RNA variants the product ends exhibit 2 nt 3′-overhangs. We conclude that full W−C base pairing at the target site is not strictly required for double-strand cleavage and that the conserved pattern of product ends is also maintained for the symmetric internal loop substrates.

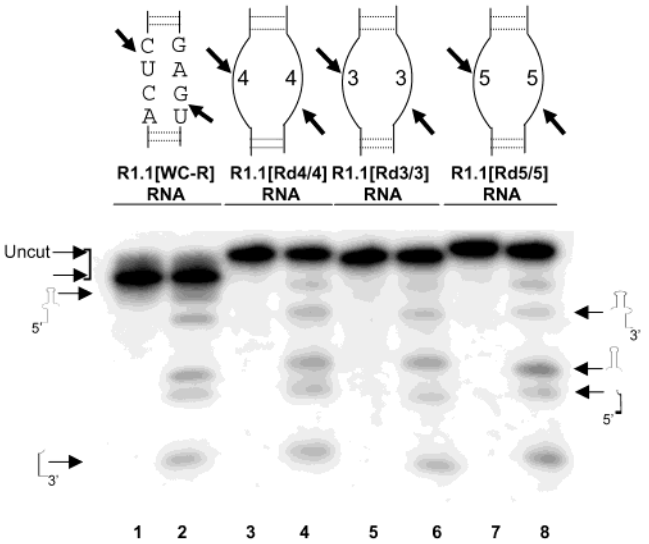

FIGURE 7: RNase III cleavage reactivities of R1.1 RNA variants containing sequence-randomized symmetric internal loops. Shown at the top of the figure are the sequences and general structures of the internal loops of R1.1[WC-R] RNA, R1.1[Rd4/4] RNA, R1.1-[Rd3/3] RNA, and R1.1[Rd5/5] RNA. RNAs were synthesized in internally ^{32}P-labeled form as described in Experimental Procedures. The RNAs were incubated with RNase III (10 nM) for 2.5 min at 37 °C. Aliquots were electrophoresed in a 15% polyacrylamide gel, and the pattern was visualized by phosphorimaging. The positions of the substrate and the products of primary site cleavage within the 3′ segment of the internal loop are shown on the left. The products of cleavage at the primary site in the internal loop 5′ segment or cleavage at both sites are indicated on the right. The limited amount of substrate cleavage allowed assessment of single cleavage events rather than the products of exhaustive digestion.

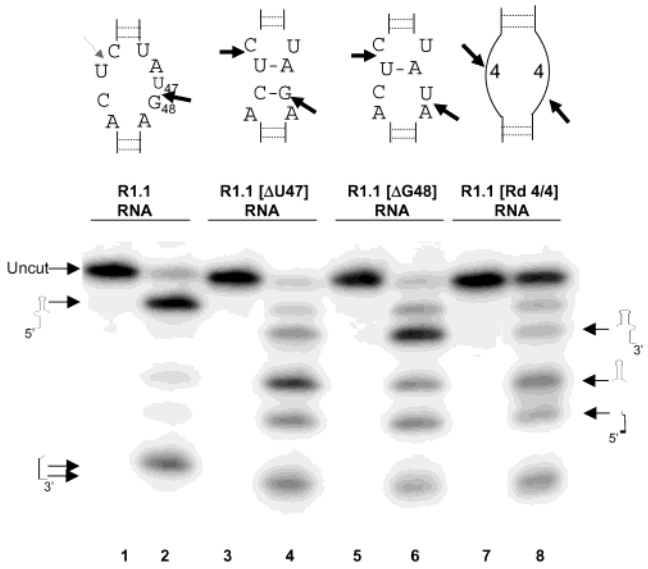

FIGURE 8: RNase III cleavage reactivities of the symmetric internal loop variants R1.1[ΔU47] RNA and R1.1[ΔG48] RNA. The internal loop sequences of R1.1 RNA, R1.1[ΔU47] RNA, R1.1[ΔG48] RNA, and R1.1[Rd4/4] RNA are shown at the top of the diagram. RNAs were synthesized in internally ^{32}P-labeled form and incubated with RNase III (10 nM) for 5 min at 37 °C. Aliquots were electrophoresed in a 15% polyacrylamide gel as described in Experimental Procedures and the reaction products visualized by phosphorimaging. The left-hand side of the phosphorimage indicates the positions of uncut substrate and the products of cleavage at the primary site (indicated by the solid arrow). The right-hand side indicates the positions of the products of cleavage within the internal loop 5′ segment or the products of cleavage at both sites.

DISCUSSION

This study has characterized an RNA internal loop that functions as a reactivity epitope in specific substrates of *E. coli* RNase III. The [4/5] internal loop in T7 RNase III substrates directs the enzymatic cleavage of a single phosphodiester within the internal loop 3′ segment. The pattern of cleavage is determined primarily by the [4/5] asymmetry rather than a stable local structure or specific nucleotide sequence. Thus, [3/4] or [5/6] internal loops confer qualitatively different cleavage patterns, and R1.1 RNA variants containing symmetric internal loops undergo cleavage of both strands. In the latter case, cleavage provides product ends with 2 nt 3′-overhangs, which is characteristic of the action of RNase III orthologues on dsRNA (*6*). A [2/2] internal loop within the precursor of the small cytoplasmic (sc) RNA of *Bacillus subtilis* is cleaved on both strands by the *B. subtilis* enzyme (*32*), and the yeast U5 snRNA precursor contains a symmetric internal loop that is also cleaved on both strands by the yeast RNase III orthologue, Rnt1p (*33*). These data provide additional support for the notion that W−C base pairing at the target site is not strictly required for double-strand cleavage.

The absence of a local tertiary structure for the R1.1 internal loop is consistent with the destabilizing effect of the motif on a 16 bp duplex. The internal loop-containing duplex is ~2.6 kcal/mol less stable than the fully W−C base-paired duplex, which formally reflects a difference of two hydrogen bonds. The absence of stable folding would enable the internal loop to adopt different conformations, which may be a key feature in constraining cleavage to a single strand. The RNA intercalating agent ethidium bromide binds to a site in the R1.1 internal loop and blocks cleavage without inhibiting RNase III recognition (*34*). It has been proposed that intercalation of the ethidium cation may stabilize an unreactive conformation (*34*).

The mechanism by which the [4/5] internal loop directs the cleavage of a single phosphodiester in the 3′-proximal segment is not known. The extra, formally unpaired nucleotide in the 3′-proximal segment is involved, since a [4/5] → [4/4] conversion of the internal loop is sufficient to promote a ss → ds shift in cleavage pattern. It has been proposed (*15*) that T7 RNase III substrates exhibit "dsRNA mimicry," wherein the internal loop possesses a quasi-double-helical structure that is recognized by RNase III but subverts the normal pattern of double-strand cleavage. Two mechanisms may be proposed for internal loop function on the basis of the observations that (i) cleavage of the two strands of a dsRNA substrate is a nonconcerted process (*12*, *16*) and (ii) a conformational change occurs in the RNase III−R1.1 RNA complex during catalysis (*35*). In one mechanism, the 5 nt, 3′-proximal strand of the internal loop is preferentially positioned in the active site, such that it is the only strand to undergo cleavage. Alternatively, if the proposed dual catalytic mechanism for RNase III (*36*) applies, both strands may be positioned in the active site, but only one of the two catalytic chemistries would occur, preferentially cleaving the 5 nt strand. In either mechanism a conformational change would follow the hydrolysis step, causing product release instead of a second catalytic event. Whatever the precise mechanism, it should be noted that the [4/5] motif is not unique in its ability to limit cleavage to the 3′-proximal segment of hairpin

substrates, as the reactivity patterns of the T7 R1.0 substrate (which contains a [2/3] internal loop; see Figure 1) and the R1.3 substrate (which contains a mismatch) exhibit the same pattern of cleavage.

RNase III cleavage sites are determined by the position of the enzyme binding site, which in turn is established by double-helical sequence elements (*16*, *27*, *29*). In this regard, RNase III recognition of substrate shares a degree of similarity to other double-strand-specific endonucleases, such as the type II restriction enzymes (*37*, *38*). Converting the R1.1 internal loop to fully W−C base-paired form does not alter the target site but merely allows the second strand to be cleaved (*27*). The internal loop can be regarded as a "second-order" reactivity epitope in its ability to control the pattern of cleavage rather than establishing reactivity per se.

RNase III substrates occur in transcripts of other members of the T7 phage group, including T3 (*39*), which suggests a conserved function(s) for RNase III in the strategy of infection characteristic of this phage group. The T7 mRNAs are significantly more stable than a typical host mRNA (*40*), which serves to maximize phage protein synthesis and reproductive efficiency. As mentioned, RNase III cleavage of the [4/5] internal loop-containing substrates in the polycistronic precursors provides 3′-hairpins that protect the upstream sequences, as well as allowing independent translation of the mature mRNAs. Although T7 mRNAs can undergo 3′-end polyadenylation (*41*), which is known to potentiate efficient degradation of bacterial mRNAs, the 3′-hairpins nonetheless provide an effective barrier to 3′−5′ exonucleases (*18*−*21*).

Why do the internal loops of T7 RNase III substrates exhibit sequence conservation, if a specific sequence is not necessary for reactivity? The canonical sequence may provide optimal cleavage efficiency, although many other variants are comparably reactive. The conservation may reflect the outcome of selective pressure on the T7 genome, including avoidance of host restriction enzymes (*42*−*44*). Also, T7 RNase III substrates may participate in other processes. For example, there is evidence that at least one of the T7 early RNase III substrates may function as a host transcription terminator or pause site, under specific conditions (*45*). The host RNA polymerase and RNase III are both modified by phosphorylation during T7 infection (*46*), which also may play a role in the observed transcriptional effect (*45*). A possible role for (phosphorylated) RNase III in transcription termination could involve cleavage of the hairpin structure within a paused host RNA polymerase−template complex.

The eight T7 RNase III processing substrates exhibit some variation in sequence and secondary structure, suggesting a degree of functional specialization. The R1.3 substrate contains a base mismatch instead of the [4/5] internal loop and can undergo either single cleavage in the 3′-strand or cleavage of both strands, with the former pathway preferred (*47*). Translation of the 1.1 and 1.2 cistrons upstream of the R1.3 substrate is dependent upon cleavage of both strands, which apparently uncovers a 1.1 gene ribosome binding site (*47*). A similar mechanism has been proposed for cleavage of the R0.3 substrate, which enhances 0.3 protein synthesis (*48*). It is possible that the in vivo recognition and cleavage of RNase III substrates is responsive to physiological changes (e.g., see refs *17* and *47*), thereby conferring a regulatory function.

The R1.1 internal loop can function as a discrete modular unit. For example, changing the internal loop to a [5/4] structure through a formal 180° rotation equivalently transposes the cleavage site. This behavior could be used to advantage in the design of RNAs with defined behaviors. For example, trans-acting antisense RNAs may be designed to bind to a target RNA sequence, forming an internal loop which would direct cleavage of only the target strand, thereby allowing the antisense strand to recycle. Second, highly stable mRNAs may be expressed in vivo which carry a 3′-stabilizing hairpin as well as a 5′-stabilizing hairpin (*49*, *50*), with each structure provided by cleavage of RNase III substrates containing [4/5] and [5/4] internal loops, respectively. The sequence flexibility of the internal loop and flanking helical elements would allow the placement of an RNase III cleavage site within a coding sequence, such that cleavage would directly inactivate the mRNA and downregulate protein production. An example of such negative regulation has been described (*51*). As the directed engineering of cellular metabolic pathways is now taking into account mRNA stability as well as translational efficiency (e.g., see refs *52* and *53*), specifically designed RNase III substrates should provide useful structures for controlling RNA stability and function.

ACKNOWLEDGMENT

The authors thank Nils Walter (University of Michigan) for advice on RNA structure probing with terbium ion and Wei Liao for preliminary studies on this project. The authors are also grateful to other members of the laboratory for their advice and encouragement.

REFERENCES

1. Belasco, J. G., and Brawerman, G., Eds. (1993) *Control of Messenger RNA Stability*, Academic Press, New York.
2. Grunberg-Manago, M. (1999) *Annu. Rev. Genet. 33*, 193−227.
3. Deutscher, M. P. (2000) *Prog. Nucleic Acid Res. Mol. Biol. 66*, 67−105.
4. Kushner, S. R. (2002) *J. Bacteriol. 184*, 4658−4665
5. Brewer, G. (2002) *Ageing Res. Rev. 1*, 607−625.
6. Nicholson, A. W. (2003) in *RNA Silencing* (Hannon, G., Ed.) Cold Spring Harbor Press, Cold Spring Harbor, NY (in press).
7. Lamontagne, B., Larose, S., Boulanger, J., and Elela, S. A. (2001) *Curr. Issues Mol. Biol. 3*, 71−78.
8. Bernstein, E., Caudy, A. A., Hammond, S. M., and Hannon, G. J. (2001) *Nature 409*, 363−366.
9. Hutvagner, G., McLachlan, J., Pasquinelli, A. E., Balint, E., Tuschl, T., and Zamore, P. D. (2001) *Science 293*, 834−838.
10. Ketting, R. F., Fischer, S. E. J., Bernstein, E., Sijen, T., Hannon, G. J., and Plasterk, R. H. (2001) *Genes Dev. 15*, 2654−3584.
11. Court, D. (1993) in *Control of Messenger RNA Stability* (Belasco, J. G., and Brawerman, G., Eds.) pp 71−116, Academic Press, New York.
12. Nicholson, A. W. (1999) *FEMS Microbiol. Rev. 23*, 371−390.
13. Robertson, H. D., Webster, R. E., and Zinder, N. D. (1968) *J. Biol. Chem. 243*, 82−91.
14. Dunn, J. J. (1982) in *The Enzymes* (Boyer, P., Ed.) pp 485−499, Academic Press, New York.
15. Robertson, H. D. (1982) *Cell 30*, 669−672.
16. Zhang, K., and Nicholson, A. W. (1997) *Proc. Natl. Acad. Sci. U.S.A. 94*, 13437−13441.
17. Dunn, J. J. (1976) *J. Biol. Chem. 251*, 3807−3814.
18. Dunn, J. J., and Studier, F. W. (1983) *J. Mol. Biol. 166*, 477−535.
19. Panayotatos, N., and Truong, K. (1985) *Nucleic Acids Res. 13*, 2227−2240.
20. Higgins, C. F., McLaren, R. S., and Newbury, S. F. (1988) *Gene 72*, 3−14.

21. McLaren, R. S., Newbury, S. F., Dance, G. S. C., Causton, H. C., and Higgins, C. F. (1991) *J. Mol. Biol. 221*, 81−95.
22. Amarasinghe, A. K., Calin-Jageman, I., Harmouch, A., Sun, W., and Nicholson, A. W. (2001) *Methods Enzymol. 342*, 143−158.
23. Grodberg, J., and Dunn, J. J. (1990) *J. Bacteriol. 170*, 1245−1253.
24. He, B., Rong, M., Lyakhov, D., Gartenstein, H., Diaz, G., Castagna, R., McAllister, W. T., and Durbin, R. K. (1997) *Protein Expression Purif. 9*, 142−151.
25. Nicholson, A. W., Niebling, K. R., McOsker, P. L., and Robertson, H. D. (1988) *Nucleic Acids Res. 16*, 1577−1591.
26. Chelladurai, B. S., Li, H., and Nicholson, A. W. (1991) *Nucleic Acids Res. 19*, 1759−1766.
27. Chelladurai, B. S., Li, H., Zhang, K., and Nicholson, A. W. (1993) *Biochemistry 32*, 7549−7558.
28. Schweisguth, D. C., Chelladurai, B. S., Nicholson, A. W., and Moore, P. B. (1994) *Nucleic Acids Res. 22*, 604−612.
29. Li, H., and Nicholson, A. W. (1996) *EMBO J. 15*, 101−113.
30. Hargittai, M. R., and Musier-Forsythe, K. (2000) *RNA 6*, 1672−1680.
31. Walter, N. G., Yang, N., and Burke, J. M. (2000) *J. Mol. Biol. 298*, 539−555.
32. Oguro, A., Kakeshita, H., Makamura, K., Yamane, K., Wang, W., and Bechhofer, D. H. (1998) *J. Biol. Chem. 273*, 19542−19547.
33. Chanfreau, G., Abou Elela, S, Ares, M., and Guthrie, C. (1997) *Genes Dev. 11*, 2741−2751.
34. Calin-Jageman, I., Amarasinghe, A. K., and Nicholson, A. W. (2001) *Nucleic Acids Res. 29*, 1915−1925.
35. Campbell, F. E., Cassano, A. G., Anderson, V. E., and Harris, M. E. (2002) *J. Mol. Biol. 317*, 21−40.
36. Blaszczyk, J., Tropea, J. E., Bubunenko, M., Routzahn, K. M., Waugh, D. S., Court, D. L., and Ji, X. (2001) *Structure 9*, 1225−1236.
37. Perona, J. J. (2002) *Methods 28*, 353−364.
38. Roberts, R. J., and Macelis, D. (2001) *Nucleic Acids Res. 29*, 268−269.
39. Pajunen, M. I., Elizondo, M. R., Skurnik, M., Kieleczawa, J., and Molineux, I. (2002) *J. Mol. Biol. 319*, 1115−1132.
40. Summers, W. C. (1970) *J. Mol. Biol. 51*, 671−678.
41. Johnson, M. D., Popowski, J., Cao, G.-J., Shen, P., and Sarkar, N. (1998) *Mol. Microbiol. 27*, 23−30.
42. Sharp, P. M., Rogers, M. S., and McConnell, D. J. (1985) *J. Mol. Evol. 21*, 150−160.
43. McClelland, M. (1985) *J. Mol. Evol. 21*, 317−322.
44. Sharp, P. M. (1986) *Mol. Biol. Evol. 3*, 75−83.
45. Ponta, H., Rahmsdorf, H. J., Pai, S. H., Hirsch-Kaufmann, M., Herrlich, P., and Schweiger, M. (1974) *Mol. Gen. Genet. 134*, 281−297.
46. Mayer, J. E., and Schweiger, M. (1983) *J. Biol. Chem. 258*, 5340−5343.
47. Saito, H., and Richardson, C. C. (1981) *Cell 27*, 533−542.
48. Studier, F. W., Dunn, J. J., and Buzash-Pollert, E. (1979) in *From Gene to Protein: Information Transfer in Normal and Abnormal Cells* (Russell, T. R., Brew, K., Farber, H., and Schultz, T., Eds.) pp 261−269, Academic Press, New York.
49. Bechhofer, D. (1993) in *Control of Messenger RNA Stability* (Belasco, J. G., and Brawerman, G., Eds.) pp 31−52, Academic Press, New York.
50. Carrier, T. A., and Keasling, J. D. (1999) *Biotechnol. Prog. 15*, 58−64.
51. Koraimann, G., Schroller, C., Graus, H., Angerer, D., Teferle, K., and Hogenauer, G. (1993) *Mol. Microbiol. 9*, 717−727.
52. Smolke, C. D., Martin, V. J., and Keasling, J. D. (2001) *Metab. Eng. 3*, 313−321.
53. Smolke, C. D., and Keasling, J. D. (2002) *Biotechnol. Bioeng. 80*, 762−776.
54. Cruz-Reyes, J., Piller, K. J., Rusche, L. N., Mukherjee, M., and Sollner-Webb, B. (1998) *Biochemistry 37*, 6059−6064.

BI030004R